

Expression of Pluripotency Markers in Nonpluripotent Human Neural Stem and Progenitor Cells

Per Henrik Vincent,¹ Eirikur Benedikz,² Per Uhlén,³ Outi Hovatta,⁴ and Erik Sundström^{1,5}

Nonpluripotent neural progenitor cells (NPCs) derived from the human fetal central nervous system were found to express a number of messenger RNA (mRNA) species associated with pluripotency, such as *NANOG*, *REX1*, and *OCT4*. The expression was restricted to small subpopulations of NPCs. In contrast to pluripotent stem cells, there was no coexpression of the pluripotency-associated genes studied. Although the expression of these genes rapidly declined during the in vitro differentiation of NPCs, we found no evidence that the discrete expression was associated with the markers of multipotent neural stem cells (CD133⁺/CD24^{lo}), the capacity of sphere formation, or high cell proliferation rates. The rate of cell death among NPCs expressing pluripotency-associated genes was also similar to that of other NPCs. Live cell imaging showed that *NANOG*- and *REX1*-expressing NPCs continuously changed morphology, as did the nonexpressing cells. Depletion experiments showed that after the complete removal of the subpopulations of *NANOG*- and *REX1*-expressing NPCs, the expression of these genes appeared in other NPCs within a few days. The percentage of *NANOG*- and *REX1*-expressing cells returned to that observed before depletion. Our results are best explained by a model in which there is stochastic transient expression of pluripotency-associated genes in proliferating NPCs.

Keywords: neural stem cells, pluripotency markers, stem cell heterogeneity

Introduction

NEURAL PROGENITOR CELLS (NPCs) are directed toward the neural lineage and are multipotent, meaning that they can give rise to neurons, glia, and oligodendrocytes but not to other cell types, as opposed to pluripotent cells, such as embryonic stem cells (ESCs) or induced pluripotent stem cells (iPSCs). Pluripotency is commonly defined as an undifferentiated cell state from which cells can generate progeny of any of the three germ layers.

As a consequence, transplanted pluripotent cells give rise to teratomas containing tumor cells differentiated along ectodermal, endodermal, and mesodermal traits. We previously showed that human fetal spinal cord-derived neural progenitor cells (hscNPCs) that do not give rise to teratomas in any situation tested express messenger RNA (mRNA) of the pluripotency-associated genes *NANOG* and *OCT4*, which are otherwise characteristic of pluripotent stem cells [1].

Cultures of hscNPCs are heterogeneous with respect to various phenotypic features depending on the culture conditions. Neurosphere cultures contain small numbers of differentiated neurons and astrocytes in addition to the neural stem

cells (NSCs) [2], while adherent cultures are less heterogeneous. Among the NSCs, subpopulations of quiescent cells and actively dividing cells can be identified in vitro, as well as in the adult brain [3].

While more differentiated neural cells can be identified with cell surface markers and sorted prospectively for transplantation studies, this has been more difficult for the most immature cells. NSCs from the fetal human brain have been claimed to display a distinct surface marker profile [4], CD133⁺/CD24^{lo}/CD45⁻. Among the neural progeny of differentiated human ESCs (hESCs), the CD15⁺/CD24^{lo}/CD29^{hi} cells are believed to constitute the NSC population [5]. The membrane glycoprotein CD133 is involved in self-renewal, metabolism, differentiation, tumorigenesis, etc. (reviewed in Li [6]), and has been used by several groups as a marker to enrich for NSCs [7–10]. Based on these findings, a phase II study of the transplantation of NSCs to patients with cervical spinal cord injuries was initiated, but was recently terminated for financial reasons [11].

In the transplantation setting, pluripotent cells are a major safety concern in that they can generate tumor growth as teratomas or even malignant teratocarcinomas [12]. If

¹Division of Neurodegeneration, Center for Alzheimer Research, Department of Neurobiology, Care Sciences and Society, Karolinska Institutet, Stockholm, Sweden.

²Neurobiology Research, Institute of Molecular Medicine, University of Southern Denmark, Odense, Denmark.

³Division of Molecular Neurobiology, Department of Medical Biochemistry and Biophysics, Karolinska Institutet, Stockholm, Sweden.

⁴Department of Clinical Sciences, Intervention and Technology, Karolinska Institutet, Karolinska University Hospital Huddinge, Stockholm, Sweden.

⁵Stockholms Sjukhem, Stockholm, Sweden.

pluripotent cells are present among the cells intended for transplantation, their number may be too low to generate teratomas in experimental xenotransplantation [13] and other safety assessments, but could nevertheless create problems when applied clinically.

Since pluripotency is defined, in part, by the prospective outcome of a putative differentiation process, it is difficult to reliably visualize truly pluripotent cells. However, to identify pluripotent stem cells, the expression of pluripotency-associated genes, such as *NANOG*, *OCT4*, *REX1*, and *SOX2*, is commonly evaluated by analyzing the mRNA species [14–16], reporter genes driven by specific promoters [17], the protein products of the genes with immunohistochemistry [18], or fluorescent transgene fusion proteins [19].

NANOG is widely believed to be the most stringent of all the pluripotency-associated markers [20]. Nevertheless, in the case of iPSCs, *NANOG* seems to be insufficient as a marker for fully reprogrammed cells [21]. In addition, in ESC cultures, *NANOG* protein levels undergo slow random fluctuations, giving rise to heterogeneous cell populations without losing pluripotency, but low *NANOG* expression corresponds to a higher propensity to differentiate. When depleted of *NANOG*-positive cells by fluorescence-activated cell sorting (FACS), *NANOG*-negative ESCs revert back to being *NANOG* positive after 1–2 weeks in culture [22,23]. Together, these results indicate that *NANOG*, although arguably the most reliable pluripotency marker, is neither specific to pluripotent cells nor sensitive enough to detect all pluripotent cells.

At present, the true potency state of a cell can only be determined retrospectively. Furthermore, some multipotent adult stem cells express pluripotency-associated markers, such as human mesenchymal stem cells that express *OCT-4*, *NANOG*, *SOX-2*, and *SSEA-4* [24,25]. *OCT-4* is also expressed by a subset of adult human [26,27] and murine [28] tissue-specific progenitor cell types and even on terminally differentiated peripheral blood mononuclear cells [29]. We do not know if nonpluripotent cells that express pluripotency-associated genes possess unique features or if this expression signifies a particularly immature subpopulation.

The identity of the most immature NSC subpopulation has been widely discussed in research on heterogeneous NPC cultures [4,30–32]. If the expression of pluripotency-associated mRNA species in hscNPCs coincides with the phenotypic traits associated with stemness in NPCs, they could be part of a controlled signaling mechanism with an impact on the phenotype of the cells or just the remains of an already-terminated pluripotency signaling pathway. In either case, the expression of pluripotency-associated mRNA species may imply a cell state that is particularly immature yet not pluripotent.

To address these questions, we investigated the features of human NPCs expressing pluripotency-associated genes to determine if they are different from nonexpressing cells. We found that the low average expression of pluripotency-associated genes in cultures of human spinal cord-derived neural progenitor cells (hscNPCs) was due to the high expression of these genes that was restricted to small subpopulations of cells. The phenotype of pluripotency-associated gene-expressing hscNPCs was similar to nonexpressing hscNPCs. Morphologically, all hscNPCs constantly changed shape, extending and withdrawing cell processes. Cell sorting

experiments showed that there were no subpopulations that stably expressed these genes. The expression of the pluripotency-associated genes was apparently the result of transient stochastic expression in human NPCs.

Materials and Methods

Tissue and cell culture

Human first trimester subcortical forebrain (fbr) and spinal cord (sc) tissue was obtained from elective routine abortions (gestational age 5.5–9 weeks) with the written informed consent of the pregnant women and in accordance with the ethical permit given by the Regional Ethics Vetting Board (Stockholm, Sweden) [33]. The tissue was carefully homogenized in NS medium [1×Dulbecco's modified Eagle's medium (DMEM)/F12 (Life Technologies), 1×N-2 supplement (R&D Systems), 5 mM HEPES (Invitrogen), 0.6% w/v glucose, and 2 µg/mL heparin (Sigma)] with a glass-Teflon homogenizer.

The single-cell suspensions were transferred to NSG medium (NS medium supplemented with 20 ng/mL EGF, 20 ng/mL bFGF, and 10 ng/mL CNTF, all from R&D Systems) at a concentration of 100–200 cells/µL and incubated at 37°C in a humidified atmosphere with 5% CO₂ in culture flasks. Fresh medium was added twice a week. When passaged, the neurospheres were mechanically dissociated with TrypLE Express (Invitrogen), and single cells were reseeded in fresh medium every 7–21 days depending on growth rate and sphere size.

Adherent cultures were achieved by passaging neurospheres and seeding single cells on a polyornithine (PO)/laminin-treated surface at a concentration of 15,000–30,000 cells/cm² and cultivated in NSG medium. The PO (Sigma) was diluted 1:6 in phosphate-buffered saline (PBS), applied for 1 h, removed and allowed to dry for 10 min, and subsequently rinsed 3× with autoclaved dH₂O. Then, 1 µg of laminin-111 (Sigma) per cm² was added to the PO-treated surface in NSG medium and incubated at 37°C in a humidified atmosphere with 5% CO₂ for 24 h before use. The adherent cells were passaged by a method similar to that described for the neurospheres, using TrypLE Express-mediated dissociation from the surface and gentle mechanical trituration.

hESCs were obtained from professor Outi Hovatta, Karolinska Institutet, Karolinska University Hospital (Huddinge, Sweden), in accordance with approval from the Regional Ethics Vetting Board in Stockholm. hESCs were grown on Laminin-521 (BioLamina) in NutriStem hESC XF (Biological Industries) medium and passaged with TrypLE Select (Gibco, Invitrogen) as described elsewhere [34]. All procedures were carried out according to the principles of the Helsinki Declaration.

In vitro differentiation

Cells were plated onto poly-D-lysine- and fibronectin-coated glass slides, grown in NS medium with 10% fetal bovine serum (NS-FBS medium) and allowed to differentiate without added growth factors in a 37°C humidified atmosphere with 5% CO₂ for 12 days. The seeding cell density was 15,000 cells/cm² in NS-FBS. After 12 days, the cells were either fixed in 4% paraformaldehyde in PBS for 10 min,

rinsed thrice in PBS and analyzed by immunocytochemistry, or dissociated with TrypLE Express and further processed for flow cytometry analysis.

Lentiviral transduction

Reporter lentiviral constructs for Nanog, Rex-1, and Oct-4 and control viruses with a constitutively active promoter (EF1 α ; Allele Biotechnology, Inc.) were transduced into newly passaged adherent cell cultures. Polybrene was added at a concentration of 2 μ g/mL. A multiplicity of infection (MOI) virus ratio >3 was used, which typically yielded >95% transduction efficiency in control experiments with control viruses without a detrimental effect on cell survival or proliferation. The viruses and polybrene were removed by extensive rinsing with NSG medium after 24 h and subsequent passaging.

Reverse transcriptase-PCR

RNA was extracted using the Qiagen RNeasy Mini Kit (Qiagen) according to the manufacturer's protocol. Cells were homogenized by passage through a 20-gauge needle in lysis buffer 10 times. Then, 100 ng of RNA was used for complementary DNA (cDNA) synthesis (SuperScript III First Strand Kit; Invitrogen) using target-specific reverse primers. The cDNA sequences were obtained from GenBank. The primers were designed using Vector NTI and Primer3 software to span exon-exon boundaries and were checked for sequence homologies using NCBI BLAST (Table 1).

The reverse transcription reactions were performed at 55°C (*NANOG*, *OCT4*, *DNMT3B*, *CRIPTO*), 50°C (*GDF3*, *GAPDH*), or 51°C (*REX1*). The polymerase chain reaction (PCR) was performed with Stratagene Paq5000 DNA polymerase. The products were run on agarose gels, and single bands were obtained, cut out, purified using the QIAquick Gel Extraction Kit (Qiagen), and sequenced to confirm the identity of the original mRNA. Negative controls included "no template" and "no reverse transcriptase" samples.

Quantitative PCR

For total RNA extraction, FACS cells were homogenized in TRIzol by repeated pipetting. Chloroform was added, the samples were centrifuged at 11,900g, and the aqueous phase was obtained. Isopropanol and glycogen were used to precipitate the RNA, which was subsequently washed twice with ice cold 95% EtOH and redissolved in water. Random hexamers were used in the cDNA synthesis step for CD133- and CD24-sorted cells, and oligo-dT primers were used for the sorted reporter cells (SuperScript III First Strand Kit; Invitrogen).

The primers for quantitative PCR (qPCR) were the same as those used for normal RT-PCR with the exception of *NANOG*, for which a TaqMan assay (Applied Biosystems) was used. The qPCR analysis was performed on a 7500 Fast Real-Time PCR System (Applied Biosystems). The PCR efficiency was evaluated by a dilution series of cDNA from pooled undifferentiated hESCs HS999 and HS980 and was >90% for all primer pairs. Negative controls included "no template" and "no reverse transcriptase" samples.

GAPDH, *OCT4*, and *REX1* were analyzed with SYBR Green chemistry (Roche) with the following amplification profile: 1 cycle of 95°C for 10 min, 40 cycles of alternating 95°C for 15 s, an annealing step at 60°C for 30 s, and an elongation step at 72°C for 45 s followed by a melting curve analysis for specificity control. The TaqMan assay parameters (*NANOG*) were: 1 cycle of 95°C for 10 min, 40 cycles of alternating 95°C for 15 s, and a combined annealing and elongation step at 60°C for 1 min.

The quantification was performed using the Pfaffl method as described in Bookout et al. [35] using pooled undifferentiated hESCs HS999 and HS980 as a reference sample and *GAPDH* as a reference gene. Software-generated thresholds and Ct values for each gene were used (7500 Fast System version 2.0.3). The amplification efficiencies were obtained by running a dilution series of hESC mRNA and used to calculate relative fold induction with the formula:

$$\text{fold induction} = \frac{\text{Eamp}_t^{\Delta\text{Ct}_t(\text{control} - \text{sample})}}{\text{Eamp}_r^{\Delta\text{Ct}_r(\text{control} - \text{sample})}}$$

where

Eamp_t = amplification efficiency for the target gene = PCR efficiency for the target gene + 1

Eamp_r = amplification efficiency for the reference gene = PCR efficiency for the control gene + 1

$\Delta\text{Ct}_t(\text{control} - \text{sample})$ = cycle number at which the signal from the target gene in the control sample reaches the threshold minus the cycle number at which the signal from the target gene in the sample reaches the threshold

$\Delta\text{Ct}_r(\text{control} - \text{sample})$ = cycle number at which the signal from the reference gene in the control sample reaches the threshold minus the cycle number at which the signal from the reference gene in the sample reaches the threshold. The data analysis was performed with Microsoft Excel. The statistical analysis was performed using the Ct values (in log₂ scale).

Fluorescence-activated cell sorting

Cells were dissociated into single-cell suspensions with TrypLE Express as described above. DNase (StemCell Technologies) was added to the cell solution, which was then filtered through a 40- μ m cell strainer (BD) to minimize

TABLE 1. PRIMERS FOR REVERSE TRANSCRIPTASE-PCR

Gene	Forward	Reverse
<i>OCT4</i>	ACATCAAAGCTCTGCAGAAAGAAGCT	CTGAATACCTTCCCAAATAGAACCC
<i>CRIPTO</i>	CCATCAGGAATTTGCTCGTCCA	GAAAGGCAGATGCCAACTAGCA
<i>DNMT3B</i>	TACACAGACGTGTCCAACATGGGC	GGATGCCTTCAGGAATCACACCTC
<i>REX1</i>	GGAATGTGGGAAAGCGTTCGT	CCGTGTGGATGCGCACGT
<i>GDF3</i>	AGACTTATGCTACGTAAAGGAGCT	CTTTGATGGCAGACAGGTTAAAGTA

the risk of clogging. The cells were made fluorescent by either the transduction of lentiviral particles or by staining with the following directly conjugated antibodies: mouse IgG1 anti-CD133-PE (Miltenyi Biotec, Bisley, Surrey, UK), mouse IgG2a anti-CD24-PerCP-Cy5.5 (BD), and mouse IgG1 anti-human-CD45-PE (BD). The isotype control antibodies were mouse IgG1-PE (Miltenyi) and mouse IgG2a-PerCP-Cy5.5 (BD). Immunostained cells were incubated for 30 min on ice and washed twice in DMEM (GIBCO) without phenol red supplemented with 2 mM EDTA.

A BD FACSDiva™ I was used for sorting the cells into 96-well plates or tubes depending on the downstream application. PBS was used as the sheath fluid, and a 100- μ m nozzle with 20 PSI (pounds per square inch) sheath pressure was chosen for optimal cell survival. Typically, the acquisition rate was 500 cells per second, Purity sort mode was used for CD24/CD133 sorting, and Single Cell sort mode was used for acquisition of reporter-expressing cells. Dead cells and debris were excluded based on SYTOX® Blue (1 μ L/mL; Invitrogen) uptake and the FSC-A signal. Doublets were excluded using an FSC-H versus FSC-A dot plot diagonal gate.

Further gates were set based on the analysis of cells stained with the appropriate combinations of directly conjugated isotype controls or untransduced cells. The postsort analysis yielded 85%–95% purity for immunostained cells and 100% purity for transduced, reporter-negative, cells. The positive events among transduced cells were not subjected to postsort analysis because of their low number.

Flow cytometry

Cell suspensions were obtained in a similar manner as for FACS. A BD FACSCalibur™ flow cytometer with CellQuest™ Pro software, version 5.2.1, was used for analysis. At least 1,000 events were analyzed from each sample. Single cells were gated based on forward and side scatter, and events with a relative fluorescence intensity half a logarithmic step higher compared with the untransduced negative control cells were considered positive. Distinguishing between negative and positive events was straightforward due to the mainly binary “on OR off” nature of the reporter gene expression, further discussed below. The spectral overlap between the FL1 (green) and FL2 (orange-red) channels prevented unambiguous detection of double-positive events, which was instead performed using an Olympus inverted fluorescence microscope with cellSens Dimension software.

Fluorescence microscopy

Live and fixed cells were investigated using an inverted Olympus fluorescence microscope with cellSens Dimension software. To evaluate the existence of cells that were double positive for Nanog/Rex-1 and Oct-4/Rex-1 reporters, more than 1,000 fluorescent double-transduced cells from 14 different hscNPC cultures were examined, all of which displayed a fluorescence intensity above background in only one channel. Fixed cells on glass slides were investigated using a Nikon fluorescence microscope with OpenLab software.

Cell observer

Time-lapse fluorescence and phase-contrast images of adherent hscNPCs transduced with Nanog and Rex-1 re-

porters were obtained with a Zeiss Cell Observer system with a 10 \times objective, rendering photos with a 150 \times 120 μ m surface area (=1,388 \times 1,040 pixels \times 1.1 μ m resolution/10 \times magnification) containing between \sim 10 and 100 cells each. Locations were chosen nonrandomly where live fluorescent cells were present. The image intervals were typically 7.5 min, and the cultures were monitored for 24 h. The image analysis was performed with ImageJ using the LSM Reader plugin and with Adobe Illustrator CC.

Sphere counting

To evaluate the sphere-forming ability of cells both positive and negative for the Nanog reporter, FACS cells that formed spheres in 96-well plates were analyzed with regards to sphere number formation and individual sphere size using an Olympus IMT-2 inverted phase-contrast microscope equipped with an Olympus CMOS camera. Photos were taken of the spheres in eight predetermined positions in each well 6 and 14 days after sorting and analyzed with ImageJ using a custom-written macro (Supplementary Data; Supplementary Data are available online at www.liebertpub.com/scd).

Results

NANOG, OCT4, REX1, CRIPTO, GDF3, and DNMT3b mRNAs are all present in NPCs

In our previous study on the neural differentiation of hESCs [1], we reported that several pluripotency-associated genes were expressed at low levels in both differentiated hESCs and hNPCs derived from embryonic and fetal tissue, which by definition are not pluripotent. To investigate this more thoroughly, we first studied the expression of several genes associated with pluripotency, often used as markers of pluripotency in cells such as hESCs and iPSCs. Surprisingly, *OCT4*, *REX1*, *CRIPTO*, *GDF3*, and *DNMT3b* mRNAs were all present at levels detectable by RT-PCR in all four cases of hscNPCs (Fig. 1), as well as in the one case of cells derived from human fetal subcortical forebrain that was analyzed. Samples of all PCR products were extracted from gels and sequenced to confirm the specificity of the PCR reaction.

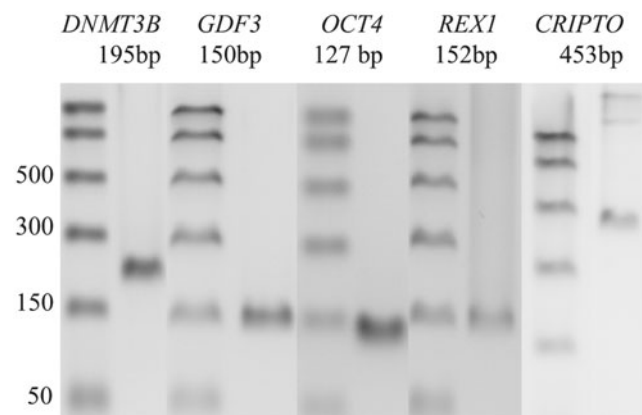


FIG. 1. PCR blots of pluripotency-associated gene transcripts in one representative hscNPC case. Ladder on the left. hscNPC, human fetal spinal cord-derived neural progenitor cell; PCR, polymerase chain reaction.

Since *NANOG* mRNA could not be detected by RT-PCR in our NPCs or in the hESCs that served as a positive control, we decided to instead use a qPCR TaqMan assay. All assays were mRNA specific, spanning at least two exons, and all PCR products were sequenced and submitted to an NCBI BLAST search to confirm the specificity of the assays. Again, using undifferentiated hESCs as control cells and GAPDH as an internal reference gene, *REX1*, *NANOG*, and *OCT4* mRNA could be detected in hscNPCs and human fetal subcortical forebrain-derived neural progenitor cells (hfbrNPCs), as well as in samples of embryonic-fetal subcortical forebrain.

The levels of all transcripts in the tissues were 20–100 times lower than in hESCs when analyzed with the Pfaffl method. With qPCR, *NANOG* mRNA was detected in 4/5 hscNPC, 3/3 hfbrNPC, and 6/6 fFbr cases; *REX1* mRNA was detected in 3/3 hscNPC, 3/3 hfbrNPC, and 3/5 fFbr cases. *OCT4* mRNA was analyzed and detected in 3/3 hscNPC cultures.

Thus, all six pluripotency-associated genes were expressed in human NPCs and in acutely isolated cells from the human fetal forebrain. While the quantification of *REX1*, *NANOG*, and *OCT4* showed much lower levels of mRNA in tissue than in hESCs, the concentration per cell would be significant if the expression occurred in a small subpopulation of NPCs.

Small subsets of NPCs express but do not coexpress NANOG, OCT4, and REX1

To determine if there were subpopulations of NPCs expressing pluripotency-associated genes, we transduced hscNPCs with lentiviral reporter constructs for *REX1*, *NANOG*, and *OCT4*. Based on the transduction of parallel cultures with a constitutively active promoter and eGFP, the transduction efficiency in hscNPCs was found to be >98%. Our data showed that the three genes were indeed expressed in small subpopulations of hscNPCs. For all reporters, a small fraction (<0.5%) of the transduced cells were distinctly fluorescent. Thirteen out of 19 hscNPC cases contained identifiable *NANOG* reporter-positive cells. Fourteen of 18 cases contained *REX1* reporter-positive cells, and 10/13 contained *OCT4* reporter-positive cells.

We confirmed the imaging data with flow cytometry analysis (Fig. 2). Similar to the microscopy results, we found highly specific expression in small subpopulations of hscNPCs. The geometric means and ranges for the non-zero values were 0.06% (0.003%–0.5%) for Rex-1, 0.1% (0.002%–0.4%) for Nanog, and 0.03% (0.003%–0.5%) for Oct-4.

To verify that the reporter gene activity accurately reflects gene transcription, we used qPCR to quantify the mRNA in cells both positive and negative for the reporter gene. The fluorescent subpopulations of Nanog, Rex-1, and Oct-4 reporter-transduced cells were isolated with FACS and subjected to qPCR analysis to confirm that the endogenous mRNA of the target genes was present in the fluorescent cells. Undifferentiated untransduced hESCs were used as control cells. The levels of *NANOG*, *REX1*, and *OCT4* mRNA were two orders of magnitude higher in fluorescent cells than in nonfluorescent cells ($n=2$). This confirmed that the reporter gene activity accurately reflected the expression of the corresponding pluripotency-associated genes.

When analyzing cells that were double transduced with combinations of reporter genes for Nanog-Rex-1 or Oct-4-Rex-1, we found that among more than 1,000 reporter-positive cells from eight different hscNPC cases, there were no cells positive for two reporter genes. This suggests that the expression of these pluripotency-associated genes does not indicate the presence of the full transcriptional loop of pluripotency.

In pluripotent cells, the expression of *NANOG*, *REX1*, and *OCT4* rapidly declines and disappears during differentiation [36]. To determine if similar changes occur in hscNPCs, we differentiated reporter gene-transduced hscNPCs for 14 days in vitro and compared them to undifferentiated hscNPCs. The proportion of Nanog and Rex-1 reporter-positive cells showed a highly significant 70%–90% decrease (Fig. 3), and although we observed a similar decrease in Oct-4 reporter-positive cells, this change was not significant due to the large variation in undifferentiated hscNPCs.

CD133⁺/CD24^{lo} sphere-forming cells do not contain more NANOG or REX1 mRNA than CD133⁻/CD24^{hi} cells

After establishing that the expression of pluripotency-associated genes occurred in small subpopulations of hscNPCs, we investigated if these subpopulations had features characteristic of multipotent NSCs. CD133⁺/CD24^{lo}/CD45⁻ cells from the human fetal forebrain constitute a sphere-forming and proliferating subpopulation in vitro, which is suggested to represent multipotent NSCs [4]. CD45 is expressed by leukocytes, which may contaminate the samples of fresh tissue, but are absent from in vitro cultures of hscNPCs at passage 1, so CD45 was omitted in our further analysis.

Using FACS, we first confirmed that CD133⁺ hscNPCs, as well as CD133⁺ cells, isolated acutely from human first trimester spinal cord and subcortical forebrain grew significantly faster than unsorted control cells (FACS flow-through), while CD133⁻ cells from spinal cord and subcortical forebrain did not form spheres.

When we analyzed the sorted cells with qPCR, *REX1* and *NANOG* mRNA were found in both CD133⁺/CD24^{lo} and CD133⁻/CD24^{hi} hscNPCs and fFbr cells (Fig. 4). The *NANOG* and *REX1* mRNA quantities did not differ significantly between sorted populations, indicating that *NANOG* and *REX1* signaling is not associated with the sphere-forming capacity of hscNPCs. Somewhat surprisingly, the mean *NANOG* mRNA concentration was actually lower in CD133⁺/CD24^{lo} hscNPCs, although this difference did not reach statistical significance ($P=0.06$) (Fig. 5).

The Nanog or Rex-1 reporter-expressing cells are not required for sphere formation

If hscNPCs that express pluripotency-associated genes were the most immature multipotent NSCs, the selective removal of these cells should eliminate the sphere-forming capacity of the cell population [4,37]. In hscNPC cultures, 50–500 spheres were formed per 10,000 cells, which were similar to the proportion of cells expressing pluripotency markers. We therefore removed all the Nanog and Rex-1 reporter-positive cells from the dissociated hscNPCs using FACS. However, we found that Nanog-/Rex-1-negative

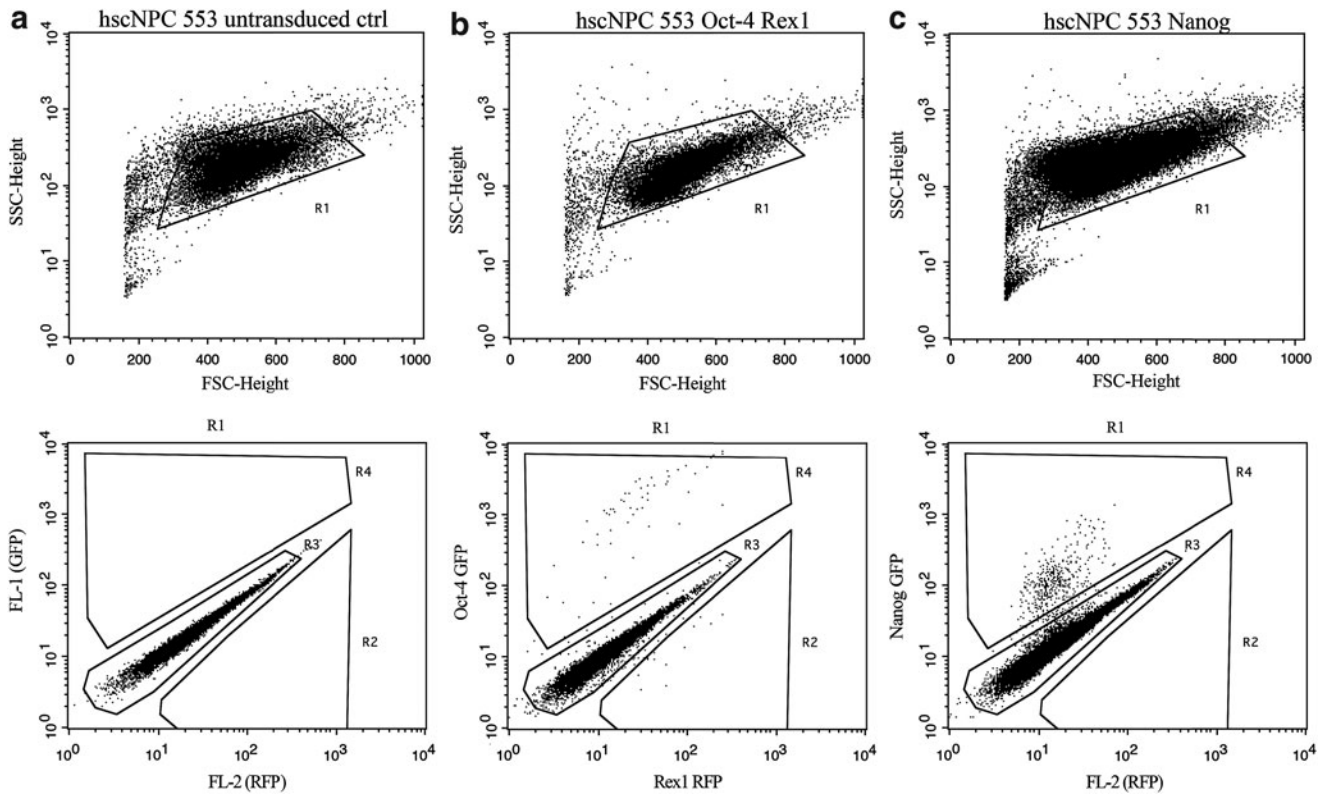


FIG. 2. Representative flow cytometry dot plots of a hscNPC case. (a–c) The gates were set to define a positive event as displaying fluorescence intensity in the plot at least half a log unit higher than background. (a) Background fluorescence of control cells. (b) Region R2 represents cells expressing RFP under the *REX1* promoter (0.07%), and R4 represents cells expressing GFP under the *OCT4* promoter (0.27%). (c) R4 represents cells expressing GFP under the *NANOG* promoter (0.45%).

hscNPCs gave rise to the same number of spheres as the FACS flow-through control cells (Fig. 6), with the same average sphere size, and the number of cells at passage 14 days later was the same. These data indicate that Nanog- and Rex-1-expressing hscNPCs do not constitute the sphere-forming stem cell population.

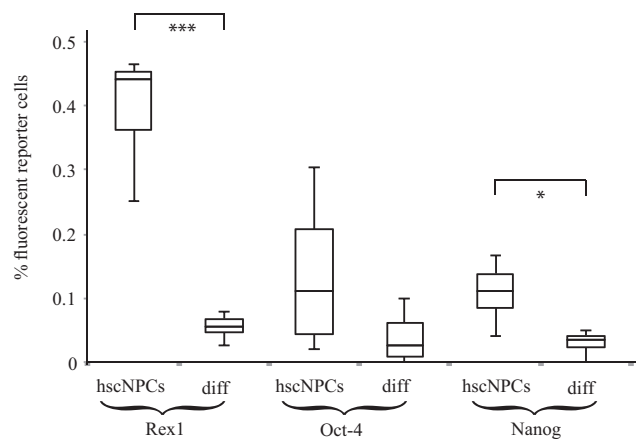


FIG. 3. Box plot of flow cytometry data showing the proportion of cells expressing the Nanog, Rex-1, and Oct-4 reporter genes in hscNPC cultures before and after differentiation in vitro. * $P < 0.05$, *** $P < 0.001$ paired *t*-test with Holm-Bonferroni's correction for multiple comparisons. Error bars represent standard deviation. $n = 4$.

A direct analysis of the sphere-forming capacity of isolated Nanog- and Rex-1-expressing hscNPCs was not possible since the plating density we could achieve with the relatively few sorted cells was too low for the survival of all NPCs tested, both as spheres and as adherent cultures. In control experiments titrating the minimum cell density for NPC cultures without reporter genes, ~1,000 cells/well or more were required for survival after plating in 96-well culture plate. The very strict cell selection we used during cell sorting resulted in considerably lower cell densities.

We then decided to study hscNPC cultures depleted of Nanog- and Rex-1-expressing cells over a period of several weeks to rule out long-term effects on sphere formation. Unexpectedly, cultures of only Nanog-/Rex-1-negative hscNPCs could not be studied over time since Nanog- and Rex-1-positive cells always reappeared in these cultures within a week after these cells had been rigorously eliminated by FACS.

An immediate postsorting analysis confirmed that all Nanog- and Rex-1-positive cells had been removed, but 2–10 days later we found a partial reconstitution of the populations of Nanog- and Rex-1-expressing hscNPCs. After approximately 3 weeks, the percentage of reporter-expressing cells consistently stabilized at the same level as before sorting (and similar to flow-through controls). Thus, the expression of both reporter genes appeared in cells previously lacking the expression of these genes.

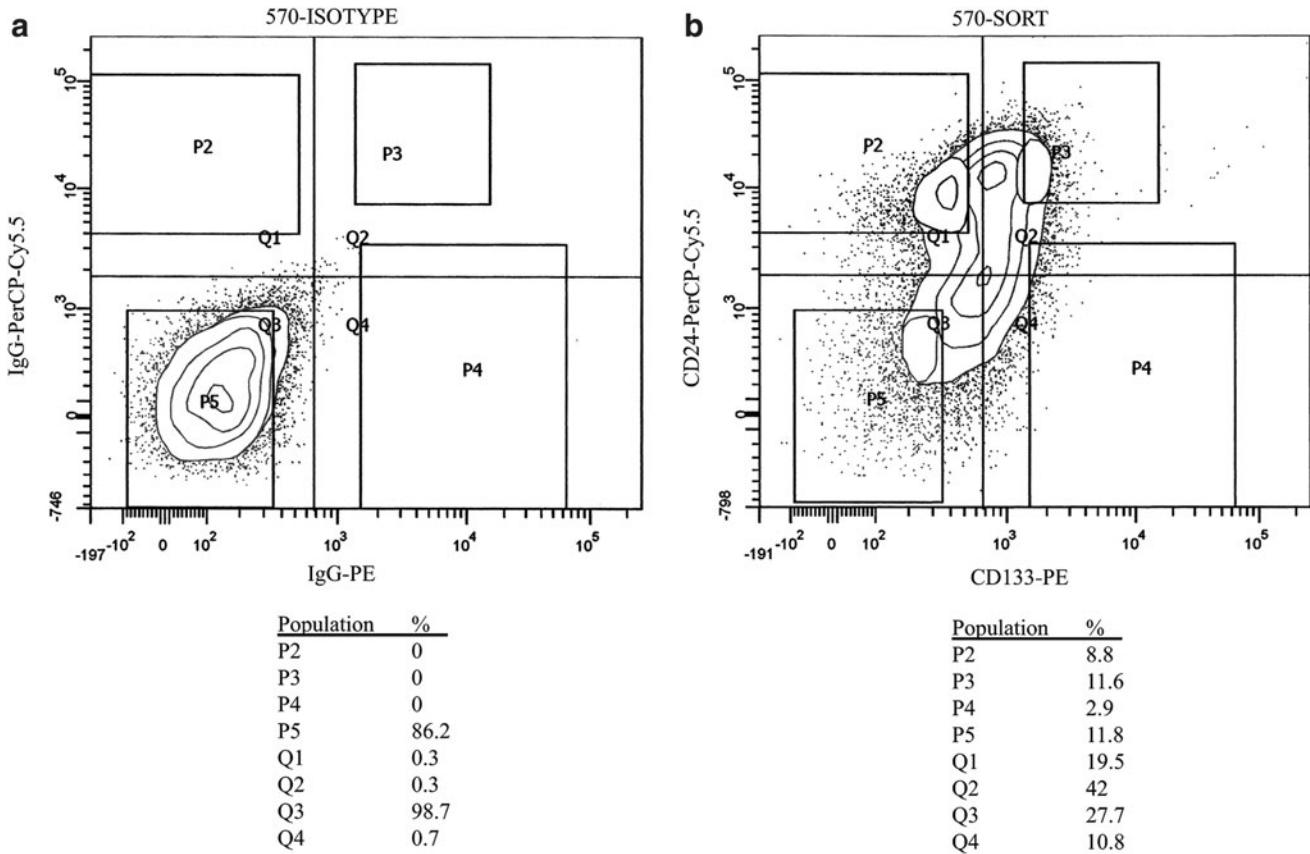


FIG. 4. FACS dot plots of a representative hscNPC culture sorted for CD24 and CD133. **(a)** Isotype background fluorescence. **(b)** Population P4 represents CD133⁺/CD24^{lo} cells, and P2 represents CD133⁻/CD24^{hi} cells. Noticeable is that the CD133⁺ population constitutes 53% of all cells. FACS, fluorescence-activated cell sorting.

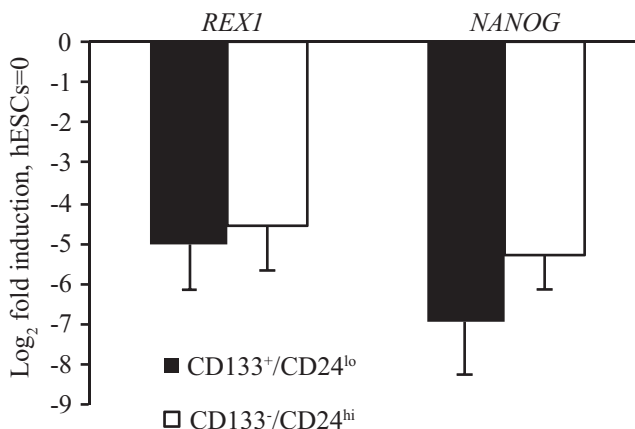


FIG. 5. Expression of *REX1* and *NANOG* mRNA in CD133⁺/CD24^{lo} and CD133⁻/CD24^{hi} hscNPCs, expressed as fold induction compared to a parallel analysis of hESCs. The *P* value for the difference between the mean *NANOG* mRNA concentrations (*P*=0.06, pairwise *t*-test with Holm-Bonferroni's postcorrection for multiple comparisons) was slightly above the preset level for significance. Error bars represent standard deviation. *n*=6. hESCs, human embryonic stem cells; mRNA, messenger RNA.

Nanog and *Rex-1* reporter-expressing and nonexpressing hscNPCs are morphologically and mitotically indistinguishable

Finally, we analyzed the morphology of adherent hscNPCs expressing reporters for pluripotency-associated genes and compared them to nonexpressing hscNPCs in the same cultures. The hscNPCs were morphologically diverse, ranging from small bipolar cells with round soma and short processes to bigger, flat stellar cells with many short protrusions or slim elongated cells with multiple, extensively branched processes. Importantly, all cells continuously switched between these morphological states (Fig. 7 and Supplementary Video S1). We found no differences in the morphology between reporter-positive cells and adjacent reporter-negative cells for any of the reporters. Before the onset of mitosis, hscNPCs retracted their processes and the cell body condensed within 15–30 min to a small spherical cell.

The reporter gene fluorescence was not reduced during mitosis, which otherwise could have explained the re-appearance of Nanog and Rex-1 reporter expression in cultures depleted of Nanog- and Rex-1-expressing hscNPCs. The progeny of a reporter gene-expressing hscNPC was always positive for the reporter (Fig. 8 and Supplementary Video S2) for up to ~20 h. Since cells expressing the pluripotency-associated genes could not be cultured in isolation, we analyzed adherent hscNPCs transduced with Nanog and Rex-1 reporter genes using live cell imaging to

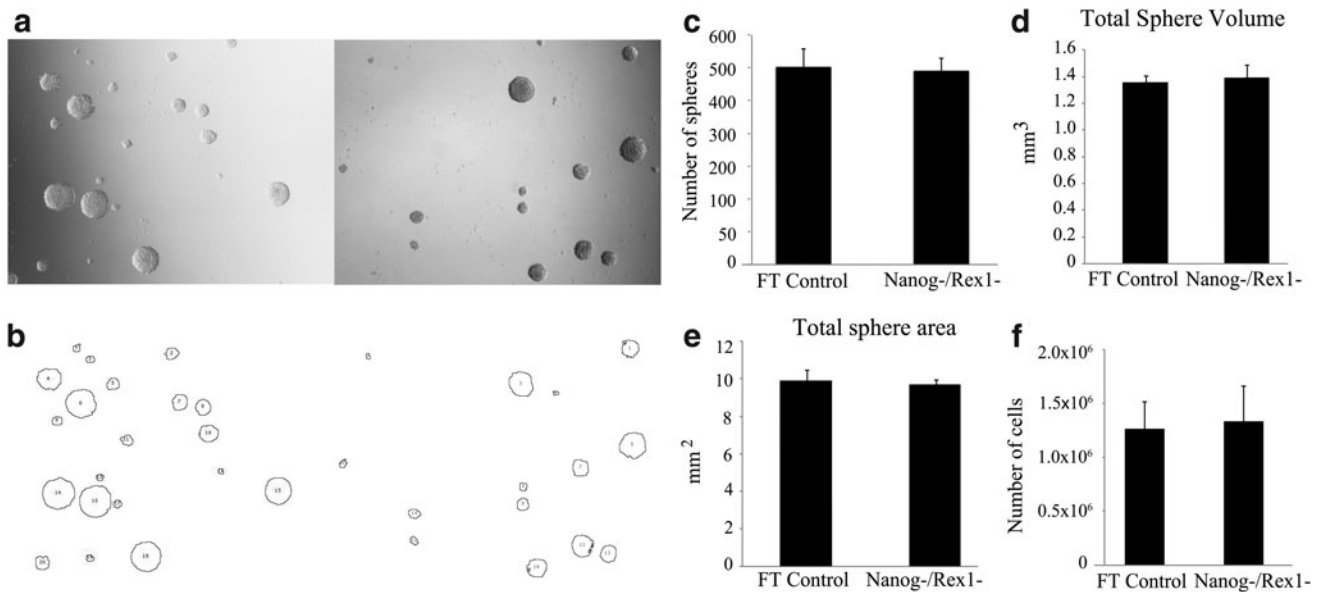


FIG. 6. Sphere-forming capacity of hscNPCs with or without the depletion of Nanog and Rex-1 reporter-expressing cells, assessed using an automated image analysis of sphere formation. (a) Phase-contrast images of spheres from control NPCs and NPCs depleted of Nanog and Rex-1 reporter-expressing cells, and (b) the digitized images used to measure: (c) the number of spheres formed, (d) the total area of the spheres in the images, (e) the total volume of spheres formed, and (f) the number of cells at first passage after plating. Error bars represent standard deviation. $n=4$. NPCs, neural progenitor cells.

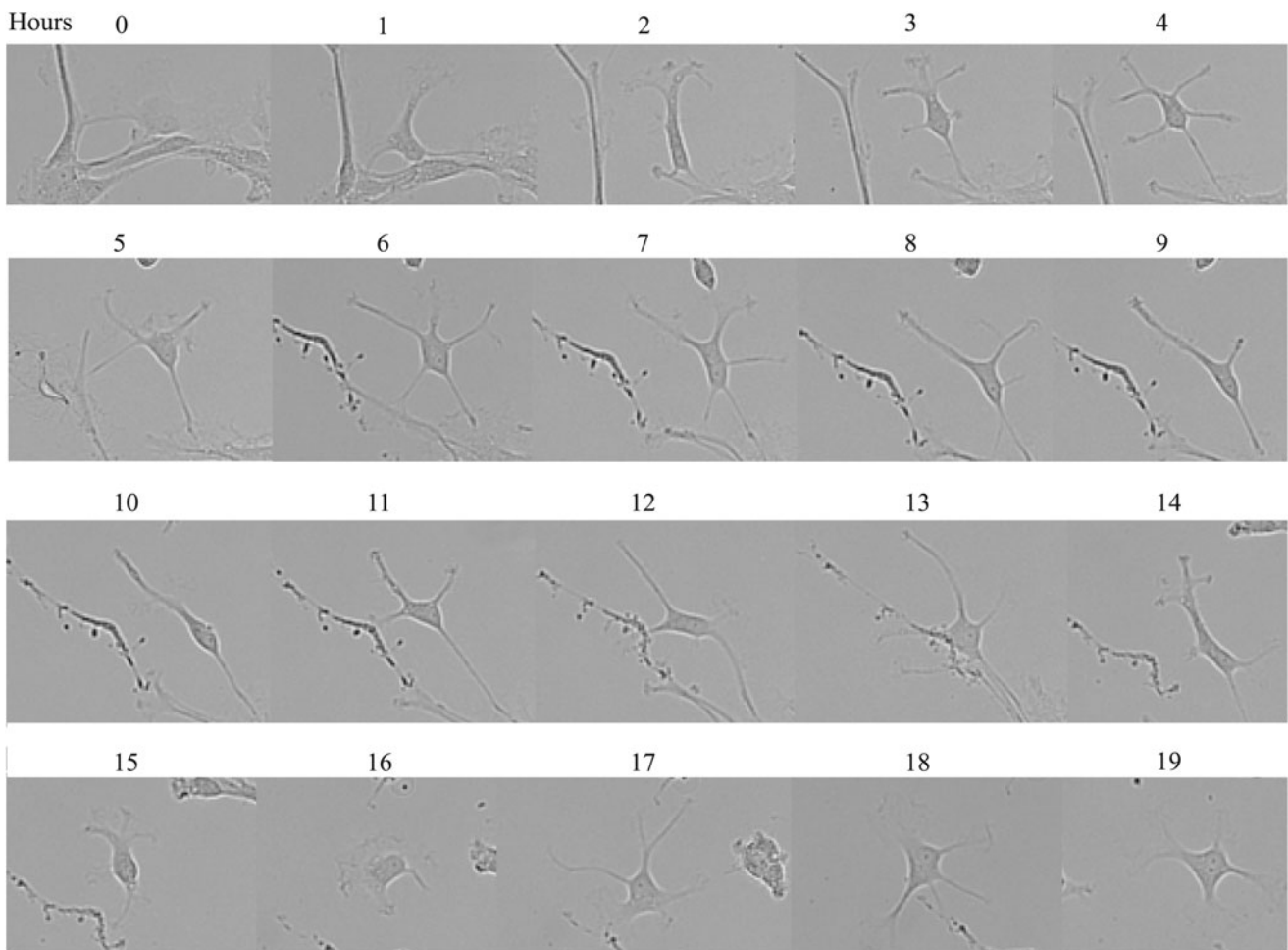


FIG. 7. Time-lapse phase-contrast images of an adherent hscNPC changing its morphology from a flat large endothelium-like cell to a cell with multiple distinct neurites to a bipolar cell, back to a flat large cell and again to a cell with distinct neurites over ~ 16 h. The time between each image was 1 h (Supplementary Video S1).

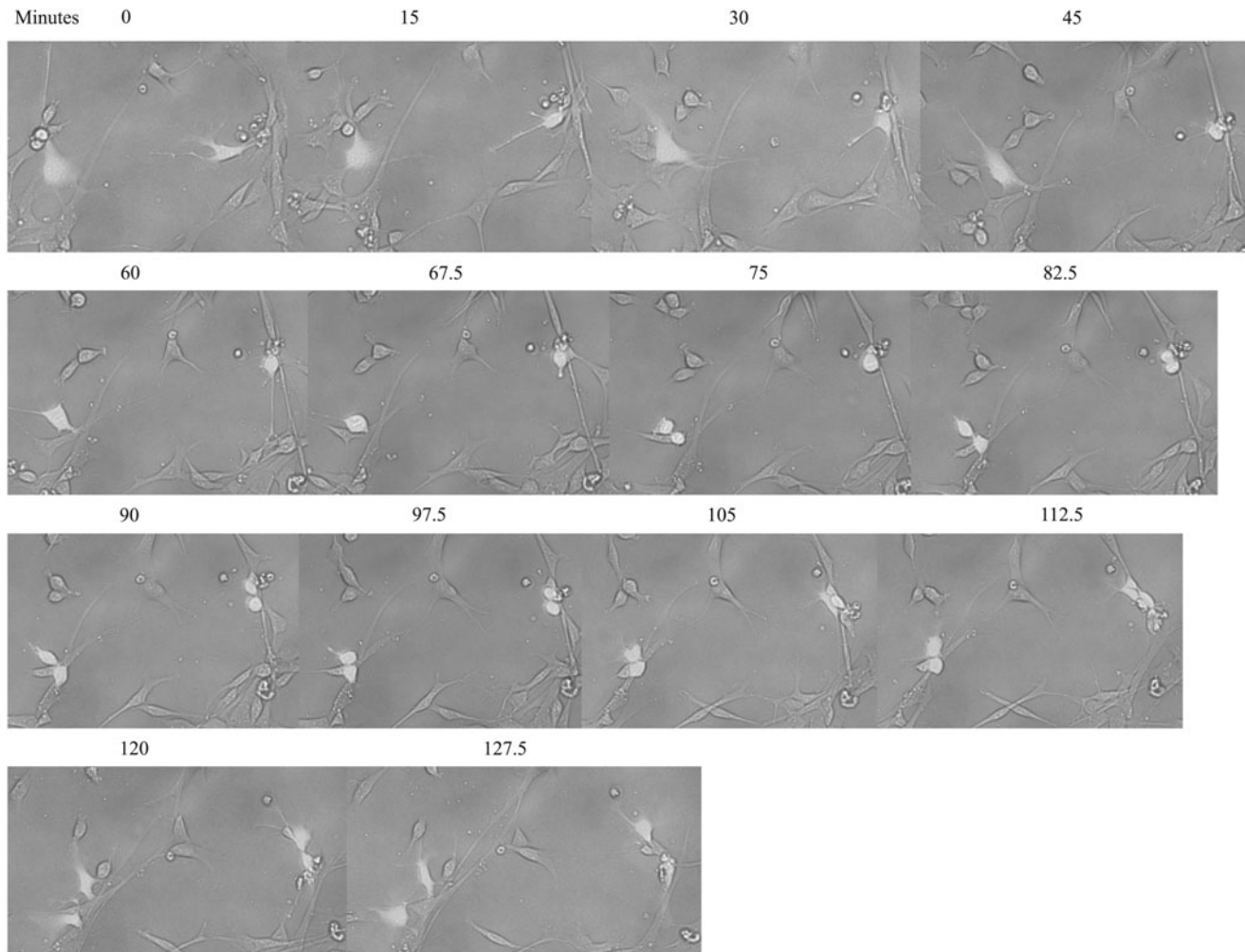


FIG. 8. Time-lapse images of two Nanog reporter-positive adherent hscNPCs dividing. The time between images was 7.5–15 min (Supplementary Video S2).

identify features unique to the hscNPCs expressing these pluripotency-associated genes. Over 24 h, we monitored 412 transduced cells from 3 different cases, of which 73 were Nanog reporter+, 107 were Rex-1 reporter+, and 232 were reporter-/-.

The frequency of cell mitosis was 5%–20% per 24 h, corresponding to a cell doubling time of 4–14 days. There was no significant difference in mitotic frequency between the reporter+ and reporter- cells ($P > 0.8$), confirming that hscNPCs expressing pluripotency-associated genes did not have a higher (or lower) proliferation rate. Cell death rates varied from 2% to 8% per 24 h between cases, with no significant difference between fluorescent and nonfluorescent cells ($P > 0.7$).

Discussion

In our previous study on human NPCs [1], we observed that a number of genes related to pluripotency (*OCT4*, *NANOG*, *GDF3*, and *DNMT3b*) were expressed in hscNPCs [1]. While all these genes gradually disappeared in hESCs during neural induction, they remained high in NPCs relative to differentiating hESCs. In the present study, we used

different approaches to analyze the features of hscNPCs that express pluripotency-associated genes.

The majority of hscNPC lines we studied showed expression of *NANOG*, *OCT4*, *GDF3*, and *DNMT3b*, confirming our previous data. In addition, *REX1* and *CRIP1*, two other genes associated with pluripotency, were also expressed in these cells. The qPCR analysis showed that the concentrations of *NANOG*, *OCT4*, and *REX1* mRNA were 15–30 times lower than in hESCs (of which $\approx 20\%$ express *NANOG*).

To address the important question whether low levels of these transcripts were present in all hscNPCs or if much higher concentrations were present in small subpopulations of cells with a specific phenotype, we transduced the cells with reporters for these three genes. The results showed that in the hscNPC cultures, a small proportion of the cells were positive for the reporters, and we confirmed that in these few cells, concentrations of transcripts were two orders of magnitude higher than in reporter-negative cells. Importantly, we found no cells with coexpression of *REX1* and *NANOG* or *OCT4*. This shows that in contrast to hESCs, the core pluripotency gene networks are not active in hscNPCs, in line with the lack of pluripotency of these phenotype-specified cells.

It should be noted that since the half-life of GFP and RFP is much longer (>24 h [38]) than, for example, *NANOG* mRNA (≈ 5 h [39]) and the *NANOG* protein (120 min in hESCs [40]), cells that turn off gene expression will remain fluorescent for some time. This does not have important consequences for the interpretation of our data. However, it will result in an overestimation of the percentage of cells expressing the pluripotency-associated genes. All hscNPC cultures expressed the pluripotency reporter genes in a small proportion of the cells, less than 0.5%. When we compared the mRNA concentrations in hscNPCs and hESCs taking the proportion of expressing cells into account, the concentrations of these mRNA species in hscNPCs were in the same range as in pluripotent hESCs.

If we also considered the longer half-life of the fluorescent reporter, the endogenous levels of the pluripotency-associated genes would be even higher, surpassing those of hESCs. However, in contrast to hESCs, the hscNPCs never coexpressed *REX1* and *NANOG* or *OCT4* and *NANOG*, which is in line with the lack of pluripotency of hscNPCs [1]. Upon the differentiation of pluripotent cells, the expression of genes associated with pluripotency is turned off, with varying kinetics [36]. We found that a similar down-regulation occurred during the differentiation of hscNPCs.

Taking these results into account, we hypothesized that although we have not previously been able to demonstrate protein expression of pluripotency-associated genes [1], the hscNPCs expressing mRNA for these genes represent the most immature cells in the heterogeneous hscNPC population, that is, the human multipotent NSCs. To address the hypothesis of pluripotency-associated genes as markers for human multipotent NSCs, we analyzed the expression of *NANOG* and *REX1* in CD133⁺/CD24^{lo} hscNPCs. This subpopulation is believed to constitute the NSC population [4], although some non-CNS stem cells coexpress CD133 and CD24 [41].

In neurosphere assays, CD133⁺/CD24^{lo} hscNPCs indeed gave rise to neurospheres that grew significantly faster than flow through control cells, similar to previously published data. However, the concentrations of *NANOG* and *REX1* mRNA were not higher in the assumed NSCs; on the contrary, the mean concentrations of *NANOG* and *REX1* mRNA were actually higher in CD133⁻/CD24^{hi} hscNPCs, although this difference did not reach statistical significance ($P=0.06$).

Further evidence against an association between pluripotency gene expression and the stem cell state of hscNPCs was acquired using *NANOG*, *OCT4*, and *REX1* reporter genes. The sphere-forming capacity of hscNPCs was not affected by the removal of all cells expressing these reporter genes. The transduction of the reporter genes under the regulation of the proximal promoter of *NANOG* recapitulates endogenous *NANOG* expression [17]. We confirmed that the endogenous mRNA levels in reporter gene-positive cells were two orders of magnitude higher compared to nonfluorescent cells, verifying that the expression of the reporter genes we used for the hscNPCs accurately represent the activation of the pluripotency-associated genes.

With the pronounced expression of genes that are critical components of pluripotency gene networks, we expected these hscNPCs to display some unique morphological features. However, when we monitored the morphology of single hscNPCs by live cell imaging over 24 h, we found

that all cells, including those expressing the pluripotency-associated genes, continuously changed their morphology. The expression of pluripotency-associated genes was not associated with any apparent features related to morphology, cell proliferation, or cell death.

It is possible that some phenotypic trait, such as the propensity to generate a certain differentiated progeny, correlates with pluripotency gene expression, as has been shown in ES cells [23]. However, it was not possible to culture isolated reporter-positive cells after sorting to allow for analysis of specific features, such as differentiation. The reason for this was that the low frequency of these cells, combined with the low yield inherent to high precision (Single Cell) sort mode FACS, resulted in too low cell densities in the plated cultures. To verify that this indeed was the reason for poor survival, we performed a control titration experiment and found that densities ~ 5 times higher than what we achieved are necessary for reliable survival of human NPCs.

Since we could not identify any particular cellular features associated with the expression of pluripotency-associated genes in NPCs, we considered if expression of pluripotency-associated genes in NPCs was a consequence of stochastic transient activation of genes. This hypothesis was confirmed in the long-term follow-up of cell depletion experiments. In all hscNPC cultures rigorously depleted of reporter gene-positive cells, we found that cells expressing the reporter genes gradually reappeared, and by three weeks the proportions of pluripotency gene-expressing hscNPCs were completely reestablished.

Taken together, our results suggest that the expression of pluripotency-associated genes in hscNPCs is not associated with a subpopulation of cells with particular features, but rather occurs in all cells, and that these genes are constantly but randomly turned on and off, although at low frequencies with short on periods. Despite a thorough reanalysis of the live cell imaging data, we did not observe any reporter gene-negative cells switching on expression. However, with only 0.2% of the cells being fluorescent at steady state, applied to a simple two-state Markov model simulation of the gradual repopulation of depleted cell cultures during two weeks, the probability of observing a single cell turning on fluorescence in a field of view with 100 cells is only $\sim 1:35$ in 24 h.

The fact that NPCs that were terminally differentiated contained lower proportions of reporter-positive cells implies that the maturity state of a cell affects the likelihood of expressing pluripotency-associated mRNA. We suggest that the probability for this type of stochastic gene expression declines as heterochromatin increases at the expense of euchromatin upon differentiation [42].

Thus, our results are best explained by transient and uncoordinated periods of pluripotency gene expression in hscNPCs that otherwise are negative for these gene transcripts. There are examples of similar situations in other cell types. Chang et al. showed that the heterogeneous population of hematological progenitor cells was restored 14–16 days after depleting them of either Sca-1-negative or Sca-1-positive cells [43]. Likewise, Gupta et al. demonstrated that a heterogeneous population of breast cancer cells containing three types of cells were restored after isolating any of the cell types [44]. In both studies, a Markov model of interchanging cell states as a result of transcriptome-wide changes could explain the results.

The transient stochastic expression of genes, and its physiological consequences, has been a major focus of gene expression studies and may explain cell heterogeneity. This was suggested to be a naturally occurring strategy to optimize population fitness in a fluctuating environment [45]. Transient expression of *REX1* similar to our results has been observed in ESCs, in which expression was associated with specification to a certain phenotype trait [46]. Also in NPCs, oscillating expression of transcription factors such as *Hes1* and *Ascl1* has been shown to control fate determination [47].

In our study, the pluripotency-associated genes analyzed did not show coordinated expression and were not associated with gross morphological changes. Further studies will show if the expression of other genes changes in concert with the pluripotency-associated genes and if this is associated with a particular phenotype.

Acknowledgments

This study was supported by Craig Hospital Foundation, Stiftelsen Stockholms Sjukhem, the Magnus Bergwall Foundation, and research funds of Karolinska Institutet.

Author Disclosure Statement

No competing financial interests exist.

References

- Sundberg M, PH Andersson, E Akesson, J Odeberg, L Holmberg, J Inzunza, S Falci, J Ohman, R Suuronen, et al. (2011). Markers of pluripotency and differentiation in human neural precursor cells derived from embryonic stem cells and CNS tissue. *Cell Transplant* 20:177–191.
- Piao JH, J Odeberg, EB Samuelsson, A Kjaeldgaard, S Falci, A Seiger, E Sundstrom and E Akesson. (2006). Cellular composition of long-term human spinal cord- and forebrain-derived neurosphere cultures. *J Neurosci Res* 84: 471–482.
- Chaker Z, P Codega and F Doetsch. (2016). A mosaic world: puzzles revealed by adult neural stem cell heterogeneity. *Wiley Interdiscip Rev Dev Biol* 5:640–658.
- Uchida N, DW Buck, D He, MJ Reitsma, M Masek, TV Phan, AS Tsukamoto, FH Gage and IL Weissman. (2000). Direct isolation of human central nervous system stem cells. *Proc Natl Acad Sci U S A* 97:14720–14725.
- Pruszak J, W Ludwig, A Blak, K Alavian and O Isacson. (2009). CD15, CD24, and CD29 define a surface biomarker code for neural lineage differentiation of stem cells. *Stem Cells* 27:2928–2940.
- Li Z. (2013). CD133: a stem cell biomarker and beyond. *Exp Hematol Oncol* 2:17.
- Barraud P, S Stott, K Mollgard, M Parmar and A Bjorklund. (2007). In vitro characterization of a human neural progenitor cell coexpressing SSEA4 and CD133. *J Neurosci Res* 85:250–259.
- Corti S, M Nizzardo, M Nardini, C Donadoni, F Locatelli, D Papadimitriou, S Salani, R Del Bo, S Ghezzi, et al. (2009). Isolation and characterization of murine neural stem/progenitor cells based on Prominin-1 expression. *Exp Neurol* 205:547–562.
- Lee A, JD Kessler, TA Read, C Kaiser, D Corbeil, WB Huttner, JE Johnson and RJ Wechsler-Reya. (2005). Isolation of neural stem cells from the postnatal cerebellum. *Nat Neurosci* 8:723–729.
- Panchision DM, HL Chen, F Pistollato, D Papini, HT Ni and TS Hawley. (2007). Optimized flow cytometric analysis of central nervous system tissue reveals novel functional relationships among cells expressing CD133, CD15, and CD24. *Stem Cells* 25:1560–1570.
- ClinicalTrials.gov. <https://clinicaltrials.gov/ct2/show/NCT02163876>, accessed May 10, 2017.
- Damjanov I and PW Andrews. (2007). The terminology of teratocarcinomas and teratomas. *Nat Biotechnol* 25:1212.
- Hentze H, PL Soong, ST Wang, BW Phillips, TC Putti and NR Dunn. (2009). Teratoma formation by human embryonic stem cells: evaluation of essential parameters for future safety studies. *Stem Cell Res* 2:198–210.
- Mitsui K, Y Tokuzawa, H Itoh, K Segawa, M Murakami, K Takahashi, M Maruyama, M Maeda and S Yamanaka. (2003). The homeoprotein Nanog is required for maintenance of pluripotency in mouse epiblast and ES cells. *Cell* 113:631–642.
- Rogers MB, BA Hosler and LJ Gudas. (1991). Specific expression of a retinoic acid-regulated, zinc-finger gene, *Rex-1*, in preimplantation embryos, trophoblast and spermatocytes. *Development* 113:815–824.
- Chambers I, D Colby, M Robertson, J Nichols, S Lee, S Tweedie and A Smith. (2003). Functional expression cloning of Nanog, a pluripotency sustaining factor in embryonic stem cells. *Cell* 113:643–655.
- Rodda DJ, JL Chew, LH Lim, YH Loh, B Wang, HH Ng and P Robson. (2005). Transcriptional regulation of nanog by OCT4 and SOX2. *J Biol Chem* 280:24731–24737.
- Lin Y, XY Li, AL Willis, C Liu, G Chen and SJ Weiss. (2014). Snail1-dependent control of embryonic stem cell pluripotency and lineage commitment. *Nat Commun* 5: 3070.
- Filipczyk A, K Gkatzis, J Fu, PS Hoppe, H Lickert, K Anastassiadis and T Schroeder. (2013). Biallelic expression of nanog protein in mouse embryonic stem cells. *Cell Stem Cell* 13:12–13.
- Silva J, J Nichols, TW Theunissen, G Guo, AL van Oosten, O Barrandon, J Wray, S Yamanaka, I Chambers and A Smith. (2009). Nanog is the gateway to the pluripotent ground state. *Cell* 138:722–737.
- Chan EM, S Ratanasirintrao, IH Park, PD Manos, YH Loh, H Huo, JD Miller, O Hartung, J Rho, et al. (2009). Live cell imaging distinguishes bona fide human iPS cells from partially reprogrammed cells. *Nat Biotechnol* 27: 1033–1037.
- Chambers I, J Silva, D Colby, J Nichols, B Nijmeijer, M Robertson, J Vrana, K Jones, L Grotewold and A Smith. (2007). Nanog safeguards pluripotency and mediates germline development. *Nature* 450:1230–1234.
- Kalmar T, C Lim, P Hayward, S Munoz-Descalzo, J Nichols, J Garcia-Ojalvo and A Martinez Arias. (2009). Regulated fluctuations in nanog expression mediate cell fate decisions in embryonic stem cells. *PLoS Biol* 7:e1000149.
- Abbaszadeh HA, T Tiraihi, A Delshad, M Saghedizadeh, T Taheri, H Kazemi and HK Hassoun. (2014). Differentiation of neurosphere-derived rat neural stem cells into oligodendrocyte-like cells by repressing PDGF- α and Olig2 with triiodothyronine. *Tissue Cell* 46:462–469.
- Trivanovic D, A Jaukovic, B Popovic, J Krstic, S Mojsilovic, I Okic-Djordjevic, T Kukulj, H Obradovic, JF Santibanez and D Bugarski. (2015). Mesenchymal stem cells of

- different origin: comparative evaluation of proliferative capacity, telomere length and pluripotency marker expression. *Life Sci* 141:61–73.
26. Tai MH, CC Chang, M Kiupel, JD Webster, LK Olson and JE Trosko. (2005). Oct4 expression in adult human stem cells: evidence in support of the stem cell theory of carcinogenesis. *Carcinogenesis* 26:495–502.
 27. Kucia M, M Halasa, M Wysoczynski, M Baskiewicz-Masiuk, S Moldenhawer, E Zuba-Surma, R Czajka, W Wojakowski, B Machalinski and MZ Ratajczak. (2007). Morphological and molecular characterization of novel population of CXCR4⁺ SSEA-4⁺ Oct-4⁺ very small embryonic-like cells purified from human cord blood: preliminary report. *Leukemia* 21:297–303.
 28. Zuba-Surma EK, M Kucia, W Wu, I Klich, JW Lillard, Jr, J Ratajczak and MZ Ratajczak. (2008). Very small embryonic-like stem cells are present in adult murine organs: ImageStream-based morphological analysis and distribution studies. *Cytometry A* 73A:1116–1127.
 29. Zangrossi S, M Marabese, M Broggin, R Giordano, M D'Erasmo, E Montelatici, D Intini, A Neri, M Pesce, P Rebulli and L Lazzari. (2007). Oct-4 expression in adult human differentiated cells challenges its role as a pure stem cell marker. *Stem Cells* 25:1675–1680.
 30. Tamaki S, K Eckert, D He, R Sutton, M Doshe, G Jain, R Tushinski, M Reitsma, B Harris, et al. (2002). Engraftment of sorted/expanded human central nervous system stem cells from fetal brain. *J Neurosci Res* 69:976–986.
 31. Cummings BJ, N Uchida, SJ Tamaki, DL Salazar, M Hooshmand, R Summers, FH Gage and AJ Anderson. (2005). Human neural stem cells differentiate and promote locomotor recovery in spinal cord-injured mice. *Proc Natl Acad Sci U S A* 102:14069–14074.
 32. Capela A and S Temple. (2002). LeX/ssea-1 is expressed by adult mouse CNS stem cells, identifying them as nonependymal. *Neuron* 35:865–875.
 33. Akesson E, JH Piao, EB Samuelsson, L Holmberg, A Kjaeldgaard, S Falci, E Sundstrom and A Seiger. (2007). Long-term culture and neuronal survival after intraspinal transplantation of human spinal cord-derived neurospheres. *Physiol Behav* 92:60–66.
 34. Rodin S, L Antonsson, C Niaudet, OE Simonson, E Salmela, EM Hansson, A Domogatskaya, Z Xiao, P Damdimopoulou, et al. (2014). Clonal culturing of human embryonic stem cells on laminin-521/E-cadherin matrix in defined and xeno-free environment. *Nat Commun* 5:3195.
 35. Bookout AL, CL Cummins, DJ Mangelsdorf, JM Pesola and MF Kramer. (2006). High-throughput real-time quantitative reverse transcription PCR. *Curr Protoc Mol Biol* Chapter 15:Unit 15.8.
 36. Ramirez JM, S Gerbal-Chaloin, O Milhavet, B Qiang, F Becker, S Assou, JM Lemaitre, S Hamamah and J De Vos. (2011). Brief report: benchmarking human pluripotent stem cell markers during differentiation into the three germ layers unveils a striking heterogeneity: all markers are not equal. *Stem Cells* 29:1469–1474.
 37. Nagato M, T Heike, T Kato, Y Yamanaka, M Yoshimoto, T Shimazaki, H Okano and T Nakahata. (2005). Prospective characterization of neural stem cells by flow cytometry analysis using a combination of surface markers. *J Neurosci Res* 80:456–466.
 38. Corish P and C Tyler-Smith. (1999). Attenuation of green fluorescent protein half-life in mammalian cells. *Protein Eng* 12:1035–1040.
 39. Sharova LV, AA Sharov, T Nedorezov, Y Piao, N Shaik and MS Ko. (2009). Database for mRNA half-life of 19 977 genes obtained by DNA microarray analysis of pluripotent and differentiating mouse embryonic stem cells. *DNA Res* 16:45–58.
 40. Ramakrishna S, B Suresh, KH Lim, BH Cha, SH Lee, KS Kim and KH Baek. (2011). PEST motif sequence regulating human NANOG for proteasomal degradation. *Stem Cells Dev* 20:1511–1519.
 41. Romagnani P and G Remuzzi. (2014). CD133⁺ renal stem cells always co-express CD24 in adult human kidney tissue. *Stem Cell Res* 12:828–829.
 42. Lee JH, SR Hart and DG Skalnik. (2004). Histone deacetylase activity is required for embryonic stem cell differentiation. *Genesis* 38:32–38.
 43. Chang HH, M Hemberg, M Barahona, DE Ingber and S Huang. (2008). Transcriptome-wide noise controls lineage choice in mammalian progenitor cells. *Nature* 453:544–547.
 44. Gupta PB, CM Fillmore, G Jiang, SD Shapira, K Tao, C Kuperwasser and ES Lander. (2011). Stochastic state transitions give rise to phenotypic equilibrium in populations of cancer cells. *Cell* 146:633–644.
 45. Acar M, JT Mettetal and A van Oudenaarden. (2008). Stochastic switching as a survival strategy in fluctuating environments. *Nat Genet* 40:471–475.
 46. Toyooka Y, D Shimosato, K Murakami, K Takahashi and H Niwa. (2008). Identification and characterization of subpopulations in undifferentiated ES cell culture. *Development* 135:909–918.
 47. Imayoshi I, A Isomura, Y Harima, K Kawaguchi, H Kori, H Miyachi, T Fujiwara, F Ishidate and R Kageyama. (2013). Oscillatory control of factors determining multipotency and fate in mouse neural progenitors. *Science* 342:1203–1208.

Address correspondence to:

Dr. Erik Sundström

Division of Neurodegeneration

Department of Neurobiology, Care Sciences and Society

Karolinska Institutet

Novum, 5th Floor

Hälsövägen 7

S14157 Huddinge

Sweden

E-mail: erik.sundstrom@ki.se

Received for publication December 8, 2016

Accepted after revision March 27, 2017

Prepublished on Liebert Instant Online March 28, 2017